IX International Conference on Particle-Based Methods
PARTICLES 2025
J. Bonet, M. Cremonesi, A. Franci, A. Gil (Eds)

# COMPUTATIONAL ANALYSIS OF CARBON-NEUTRAL BIOFUELS CO-FIRING IN A ROTARY KILN

**SH. SABERI[*, †], C. SPIJKER[†], M. GRUBER[‡], AND I. KOFLER[*]**

[*] K1-MET GmbH
Area 2, Decarbonization and Sector Coupling,
Stahlstraße 14, 4020 Linz, Austria
e-mail: shekoofeh.saberi@k1-met.com, irmela.kofler@k1-met.com, www.k1-met.com

[†] Technical University of Leoben
Chair of Thermal Processing Technology
Franz Josef-Straße 18, 8700 Leoben, Austria
email: christoph.spijker@unileoben.ac.at, www.unileoben.ac.at

[‡] RHI Magnesita GmbH
8700 Leoben, Austria
email: markus.gruber@rhimagnesita.com, www.rhimagnesita.com

**Key words:** Rotary kiln, Carbon-neutral biofuels co-firing, CFD, Particle modeling.

**Abstract.** This study presents a computational fluid dynamics (CFD) analysis of biomass co-firing in an industrial rotary kiln as a pathway toward reducing fossil fuel dependency and supporting decarbonization strategies. A three-dimensional multiphase model was developed in ANSYS Fluent, where biomass was represented as multi-component particles undergoing sequential processes of drying, pyrolysis, and char oxidation. Two operating scenarios were evaluated: (i) a baseline case with natural gas as the sole fuel, and (ii) a co-firing case in which 10% of the thermal input was provided by carbon-neutral biofuels.

The results highlight the influence of biomass addition on the thermal field and particle behavior. While a slight reduction in peak flame temperature was observed after biomass injection, the overall temperature distribution and bed heating profiles remained stable and adequate for process requirements. Particle-scale analysis confirmed complete thermal conversion, with moisture release, volatile consumption, and char oxidation leading to full burnout within the residence time.

These findings demonstrate the technical feasibility of partial biomass substitution in rotary kilns and emphasize the value of CFD modeling as a predictive tool for evaluating combustion stability, particle conversion, and process efficiency in high-temperature industrial systems.

## 1 INTRODUCTION

The European Union has started a progressive decarbonization pathway with the aim of becoming carbon neutral by 2050 [1]. The growing emphasis on meeting sustainability and climate goals to reduce $CO_2$ is one the main motivations to replace green sources of energy with fossil fuels. In recent years, many studies have been conducted to find alternative sources of

energy. At the same time, industries are aiming for economic and operational efficiency, meaning that any alternative fuel or process must also make sense financially.

There is a growing trend in industry to convert existing fossil fuel-based burners to burn other fuel types, such as agricultural residues, although whether such conversion is environmentally beneficial remains controversial. Therefore, the trend of converting the existing coal-fired power plants to biomass-fueled ones is driven by several factors, including state-level renewable portfolio standards, federal incentives and looming environmental regulations, consumer demand and environmental awareness, and the economic climate that is making coal less attractive [2].

Typical biomass fuels for power generation include wood-based fuels such as wood chips, sawdust, bark, tree trimmings, paper and cardboard; agricultural wastes such as straw, rice husks and nut shells; sludges from paper mills and municipal sources; and energy crops specially grown for use as biofuels such as switchgrass, eucalyptus, willow and poplar trees [3]. Biomass stands out as a carbon-neutral and renewable resource, making it a highly promising alternative, especially when its combustion behavior is well understood and optimized through modeling.

However, the integration of biomass into high-temperature industrial processes remains technically challenging. Carbon-neutral biofuels exhibit large variations in particle size, moisture content, and chemical composition, which affect devolatilization rates, char reactivity, and ultimately the stability of the combustion process. Compared to natural gas or coal, biomass has lower energy density and more complex thermal decomposition pathways. These features necessitate advanced numerical modeling approaches to predict its combustion behavior and to support process optimization in industrial furnaces and kilns.

Rotary kilns are of particular interest in this context as they are widely used in industries, where reliable high-temperature processing is essential. As rotating furnaces with strong coupling between gas flow, radiation, and solid bed motion, rotary kilns present a challenging environment for fuel substitution studies. Nevertheless, they also provide a unique opportunity for gradual decarbonization, as biomass can be introduced in partial replacement of conventional fuels without requiring fundamental changes to kiln operation.

Computational fluid dynamics (CFD) provides a powerful framework for studying these complex systems. Recent advances in multiphase modeling have enabled the representation of biofuel particles as multi-component systems undergoing sequential processes of drying, pyrolysis, and char oxidation. Such particle-resolved approaches allow tracking of mass loss, particle shrinkage, gas release, and heat exchange, thereby offering detailed insights into biomass conversion within industrial-scale devices.

In this study, biomass co-firing in a rotary kiln was investigated using a CFD-based approach. A detailed multiphase model was developed in ANSYS Fluent, in which carbon-neutral biofuels were introduced as representative particles. The simulations analyzed flame and bed temperature distribution, gas species evolution, and the energy release during thermal conversion, comparing baseline natural gas firing with a case where 10% of the energy input was replaced by biomass.

The results provide new insights into the feasibility of biofuels co-firing in rotary kilns, showing its potential as a carbon-neutral alternative fuel while highlighting the thermal and chemical dynamics that govern its behavior. Ultimately, this work contributes to ongoing efforts to improve biomass combustion systems, reduce environmental impacts, and support the

development of cleaner and more efficient energy technologies.

## 2 METHODOLOGIES

This study employs Computational Fluid Dynamics (CFD) to analyze the co-firing of biomass with conventional fuel in an industrial rotary kiln. The simulations are performed in ANSYS Fluent, where the gas phase is described using turbulence, combustion, and radiation models, while the solid phase is treated through a multi-component particle approach. Biofuel particles undergo sequential processes of drying, pyrolysis, and char oxidation, represented through user-defined functions (UDFs) that capture their distinct thermo-chemical behavior. By coupling gas-phase reactions with particle-scale conversion, the model provides a comprehensive framework to evaluate flame dynamics, temperature distribution, and the overall influence of biomass addition on kiln performance.

### 2.1 Computational domain

The computational domain represents a three-dimensional rotary kiln with an overall length of approximately 100 m and an internal diameter of about 3 m. The model includes multiple inlet boundaries corresponding to the supply of air and natural gas, as well as a dedicated inlet for biomass particle injection. Figure 1 shows a schematic view of the rotary kiln geometry, highlighting the main flow boundaries and outlet.

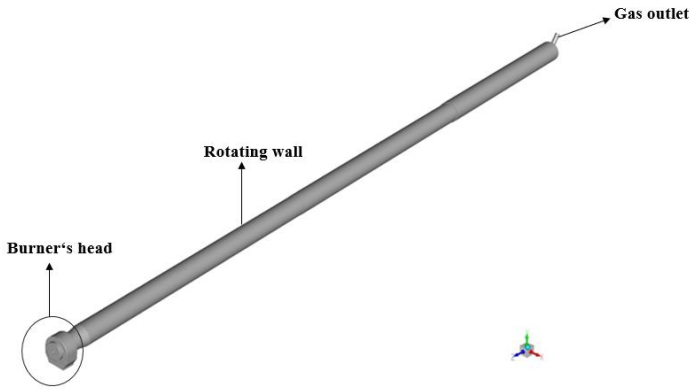


**Figure 1**: Geometry of the rotary kiln

### 2.2 Numerical framework

The simulations are carried out using a commercial CFD package, which solves the governing conservation equations for mass, momentum, energy, and chemical species in three dimensions. A steady-state Reynolds-averaged Navier–Stokes (RANS) [4] formulation is employed, with turbulence closure provided by the realizable k–ε model [5], which has been widely applied in combustion modeling. Radiative heat transfer, which plays a dominant role in rotary kilns, is described using the discrete ordinates (DO) model [6], allowing for directional dependence of radiative fluxes.

### 2.3 Gas phase modeling

The gas phase includes natural gas and air streams, with combustion described by the species transport model coupled to the eddy dissipation concept (EDC) [7] to capture turbulence–chemistry interactions. The DRM-19 reaction mechanism [8] is applied, which is suitable for hydrocarbon combustion and capable of representing light volatiles released during pyrolysis. The fuel is modeled as Austrian natural gas, with the following molar composition: $CH_4$ (97.97%), $C_2H_6$ (1.05%), $CO_2$ (0.11%), and $N_2$ (0.87%).

Thermophysical properties of the gas phase are defined consistently with the CHEMKIN [9] import setup. Gas density is evaluated using the ideal gas law, while the specific heat capacity is calculated using a mixing law based on species contributions. Thermal conductivity and viscosity are specified as constant values of 0.0454 W/m·K and $1.72\times10^{-5}$ kg/m·s, respectively.

### 2.4 Solid bed representation

The solid material within the kiln is represented as a moving bed. Its translational velocity is defined according to kiln throughput, while the kiln wall is modeled as a rotating surface to reproduce realistic boundary conditions for heat and momentum exchange. Thermal interaction between the hot gas, the refractory wall, and the solid bed is explicitly considered, ensuring a realistic prediction of bed temperature evolution.

To account for radial heat losses through the kiln lining, the refractory wall is modeled as a multi-layer system following the approach of Swaminathan et al. [10]. The overall heat transfer coefficient is determined from the series of thermal resistances across the concentric layers of refractory and insulation bricks:

$$\frac{1}{U} = \frac{1}{\lambda_1}\ln\left(\frac{r_2}{r_1}\right) + \frac{1}{\lambda_2}\ln\left(\frac{r_3}{r_2}\right) + \cdots + \frac{1}{\lambda_n}\left(\frac{r_{n+1}}{r_n}\right) \tag{1}$$

where $\lambda_i$ denotes the thermal conductivity of the i-th layer, and $r_i$, $r_{i+1}$ are the corresponding inner and outer radii. For the refractory lining, calcium oxide (CaO) is used as the representative material, with a constant density of 2000 kg/m³, a specific heat capacity of 783 J/kg·K, and a thermal conductivity of 200 W/m·K. Radiative properties are simplified by assuming zero absorption and scattering coefficients and a refractive index of unity. This formulation captures the cumulative thermal resistance of the refractory lining and ensures a realistic estimation of heat transfer between the hot gas, the bed, and the external environment.

### 2.5 Biomass particle modeling

Biomass is introduced as carbon-neutral biofuels. Particles are modeled using the Discrete Phase Model (DPM) with a multi-component particle formulation. Each particle is defined by its composition, consisting of approximately 90.7% lignin (volatile compounds and char), 6.5% moisture, and 2.8% ash.

These components undergo sequential thermal processes, including drying, pyrolysis, and char oxidation, as the particle moves through the combustion zone. To establish the kinetic parameters of these conversion steps, thermogravimetric analysis (TGA) was conducted at a heating rate of 30 K/min. From the resulting reaction rate curve (Figure 2) and the mass-loss curve (Figure 3), the characteristic stages of drying (200–400 K), pyrolysis (~600 K), and char

conversion (>650 K) were identified. By fitting the kinetic model to these experimental data, the reaction rate constants and Arrhenius parameters were extracted. This ensured that the implemented submodels for drying, pyrolysis, and char reactions are directly validated by laboratory measurements and represent the actual thermal decomposition behavior of carbon-neutral biofuels.

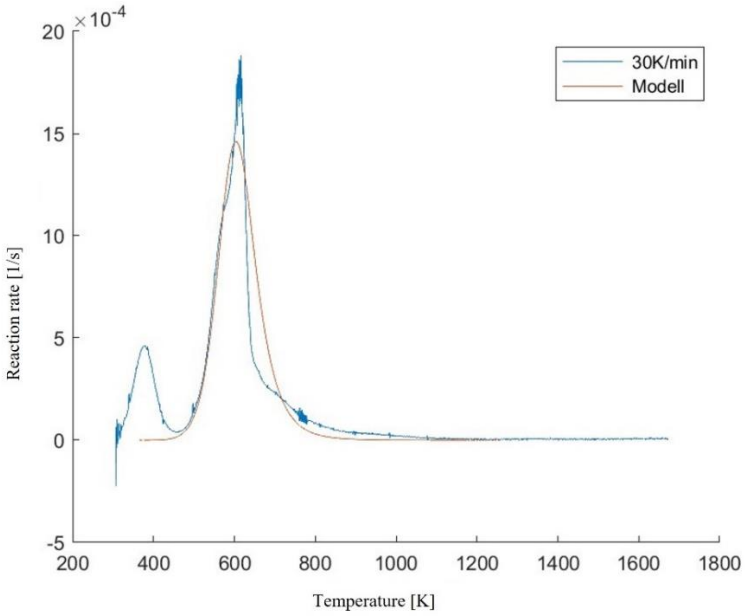


**Figure 2**: Thermogravimetric analysis (TGA) of reaction rate

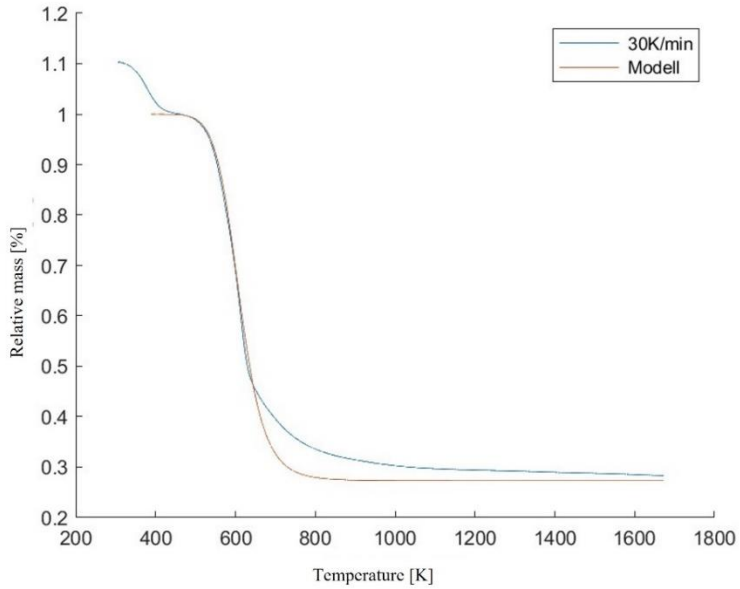


**Figure 3**: Thermogravimetric analysis (TGA) of mass loss

These thermal conversion steps are implemented as follows:

### a. Pyrolysis

Pyrolysis refers to the thermal decomposition of the lignin fraction of biofuel in an oxygen-free environment, leading to the release of volatile species and the formation of a solid char residue. This process is represented schematically as:

Lignin → Volatiles + char

The pyrolysis rate is modeled as a function of both particle temperature and composition, expressed as:

$$R_{Pyr} = A.\exp\left(-\frac{T_a}{T_P}\right).X_{Lignin}^{n}.m_P \tag{2}$$

where $T_P$ is the particle temperature, $X_{Lignin}$ is the lignin mass fraction, and $m_P$ is the particle mass. The kinetic parameters are defined using a pre-exponential factor $A=e^{13.1}$, an activation temperature $T_a$=10748K, and a reaction order of n=2. This formulation provides a more realistic description of pyrolysis by linking the reaction rate simultaneously to thermal conditions and the availability of volatile matter within the particle.

### b. Drying

Drying is modeled as a thermal phase-change process, initiated when the particle temperature $T_P$ exceeds the boiling point of water ($T_{boil}$=373K). The rate of moisture evaporation is determined from the sensible heat available above the boiling point during each time step. The heat available for evaporation, $h_{evp}$, is expressed as:

$$m_{evp} = \frac{h_{evp}}{h_{lat}\Delta T} \tag{3}$$

Where $m_{evp}$ is evaporated water mass, $m_P$ is the particle mass, $C_P$ is the particle heat capacity, $\Delta t$ is the time step, and $h_{lat}=2.2564\times10^6$ J/kg is the latent heat of vaporization. This formulation ensures that moisture release occurs only when sufficient thermal energy is available, linking the drying rate directly to particle heating dynamics.

### c. Char reaction

The residual char forms during pyrolysis participates in heterogeneous gas–solid reactions with surrounding gas-phase species such as $CO_2$, $H_2O$, and $H_2$. Three global reactions are considered [11]:

1. Bodouard reaction: $C(s)+CO_2\rightarrow 2CO$

The reaction rate is expressed as:

$$R_{BR} = A_{BR}e^{-\frac{E_{a,BR}}{RT}}\left(\frac{Y_{CO_2}}{M_{CO_2}} - \frac{Y_{CO_2}}{M_{CO}K_{BR}}\right)\rho_g RT \tag{4}$$

2. Water-gas reaction: $C(s)+H_2O\rightarrow H_2+CO$

$$R_{HW} = A_{HW}e^{-\frac{E_{a,HW}}{RT}}\left(\frac{Y_{H_2O}}{M_{H_2O}} - \frac{Y_{CO}}{M_{CO}M_{H_2}K_{HW}}\right)\rho_g RT \tag{5}$$

3. Methanation: $C(s)+2H_2\rightarrow CH_4$

$$R_M = A_M e^{-\frac{E_{a,M}}{RT}}((\frac{Y_{H_2}}{M_{H_2}})^2 \rho_g RT - \frac{Y_{CH_4}}{M_{CH_4} K_M})\rho_g RT \quad (6)$$

In these reaction rate expressions, A denotes the pre-exponential factor (reaction constant), while $E_a$ represents the activation energy in joules per mole. The universal gas constant is given by R [J/(mol·K)], and T is the local temperature in kelvin. The species mass fraction in the gas phase is denoted by $Y_i$, and $M_i$ corresponds to the molecular weight of the respective species [kg/kmol]. The equilibrium constant is represented by K, and $\rho_g$ denotes the gas density [kg/m3]. This kinetic scheme captures the main heterogeneous pathways of char consumption, linking solid carbon oxidation to the surrounding reactive environment and thereby influencing overall combustion efficiency and syngas composition.

### 2.5 Simulation cases

The numerical investigation is carried out in two stages. First, the rotary kiln is simulated under baseline conditions, i.e., without biomass injection, in order to establish the reference thermal and flow fields. Subsequently, a second case is examined where approximately 10% of the thermal input is replaced by carbon neutral biofuels. This comparative approach allows the direct evaluation of the effects of biomass addition on combustion performance, particle behavior, and the overall thermal environment of the kiln.

## 3 RESULTS AND DISCUSSION

The numerical results are presented with emphasis on two key aspects: modification of the temperature field due to biofuel co-firing, and the thermal conversion behavior of the injected particles.

Figure 4 shows the temperature of the flame after injection of biofuels. The temperature comparison before and after biofuel injection is shown in figure 5.


**Figure 4**: Flame temperature distribution after biomass injection, showing peak values near the burner (~2300–2500 K) and a gradual decrease toward the kiln outlet.

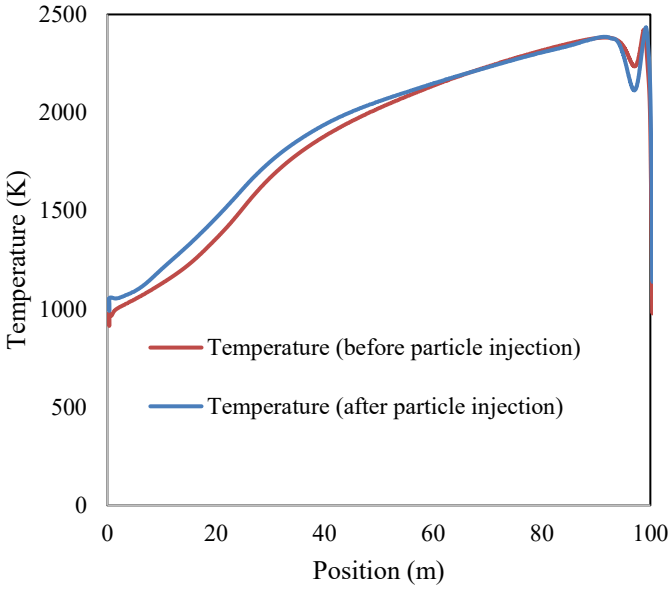


**Figure 5**: Axial gas temperature distribution along the rotary kiln for baseline and biomass co-firing cases

The temperature of the solid bed increased progressively along the kiln length in both the baseline and co-firing cases. With biofuels addition, a slight reduction in bed temperature was observed in the near-burner region due to the lower reactivity of particles during their initial heating phase. However, this difference diminished further downstream, and the outlet temperature of the bed remained within the required operational range. Figure 6 represents the material temperature. A comparison of bed temperatures before and after particle injection is presented in Figure 7.


**Figure 6**: Temperature distribution of the solid bed along the rotary kiln, showing a gradual increase from the inlet to the outlet, with maximum values near the discharge end.

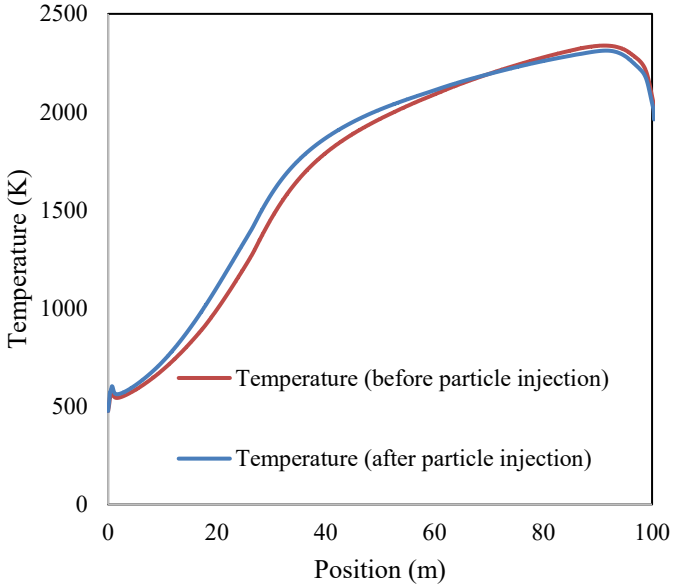


**Figure 7**: Material temperature distribution along the bed for baseline and biomass co-firing cases

Biomass particles exhibited the expected sequence of thermal conversion processes. As they entered the kiln, particle temperature rose rapidly due to convective and radiative heating. The continuous increase in particle temperature, coupled with the corresponding decrease in particle mass, confirmed complete burnout within the available residence time. The particle temperature and particles mass are shown in Figures 8 and 9, respectively. To maintain clarity, particle trajectories are excluded once the residual mass reaches 99% ash, ensuring that the analysis focuses on the active stages of thermal conversion.

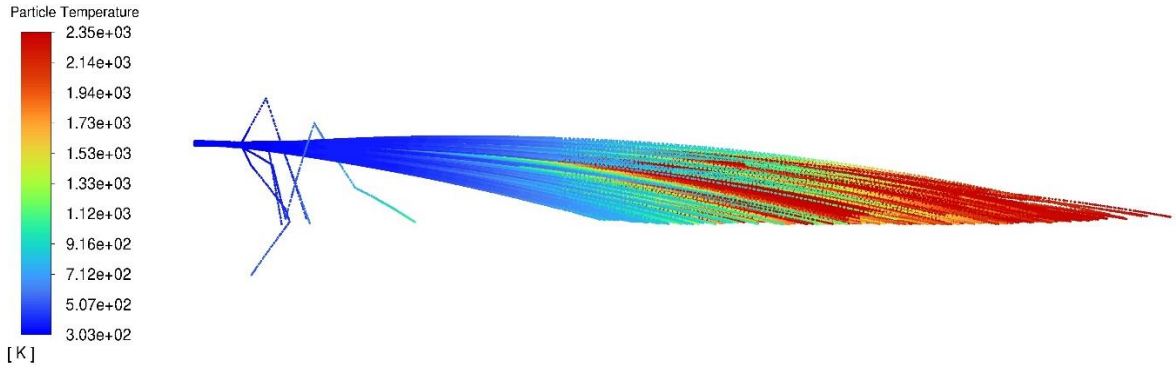


**Figure 8**: Particle temperature distribution along the kiln, showing rapid heating after injection, followed by a gradual rise toward maximum values as thermal conversion progresses.

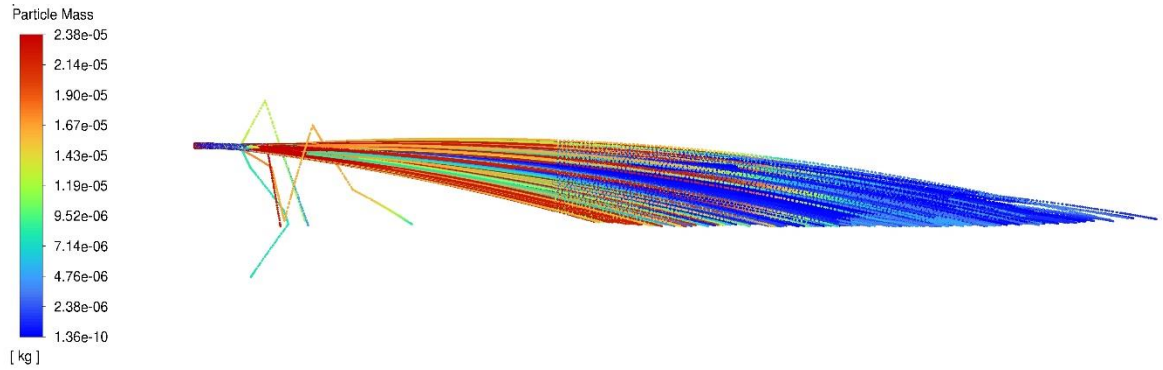


**Figure 9**: Particle mass distribution along the kiln, indicating continuous reduction during drying, pyrolysis, and char oxidation, with near-complete burnout toward the outlet.

Once the temperature exceeded the boiling point of water, moisture was released through drying. This was followed by pyrolysis, where volatile matter was consumed and char was formed. With further heating, the char fraction decreased progressively due to heterogeneous oxidation reactions until only inert ash remained. The mass fractions of lignin, water, ash, and char are shown below.

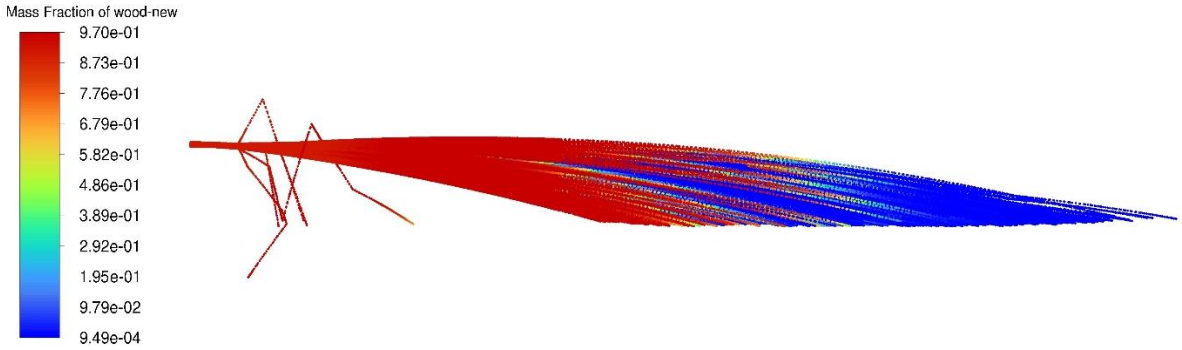


**Figure 10**: Lignin mass fraction along particle pathline, showing a progressive decrease as the biomass undergoes devolatilization and conversion to char.

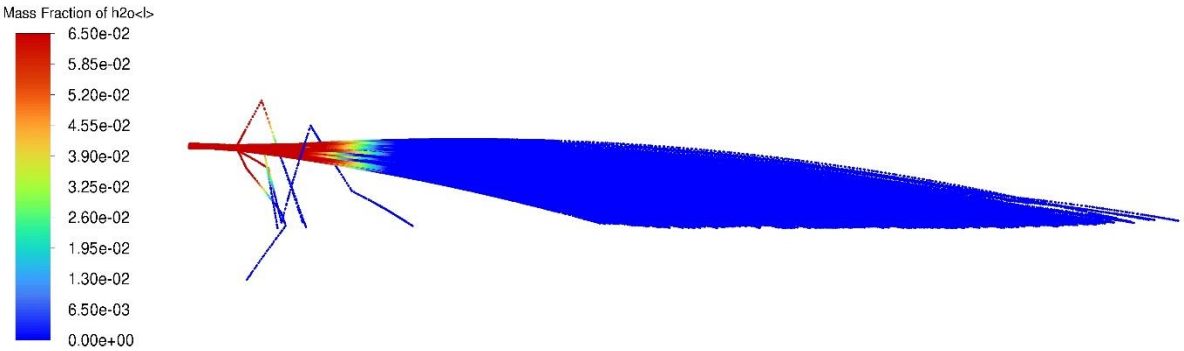


**Figure 11**: Water mass fraction distribution along particle pathline, showing rapid moisture release during the initial heating stage, followed by complete evaporation downstream.

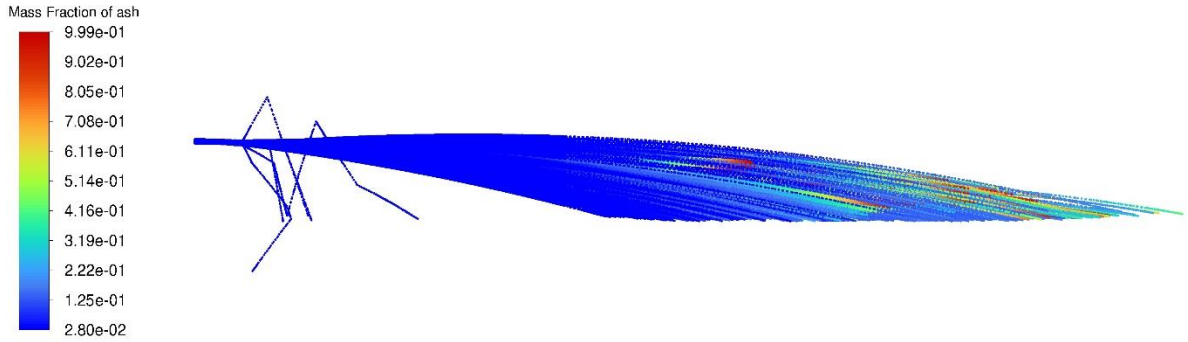


**Figure 12**: Ash mass fraction distribution, showing the progressive accumulation of inert residue as volatile and char components are consumed, with stable values reached near the kiln outlet.

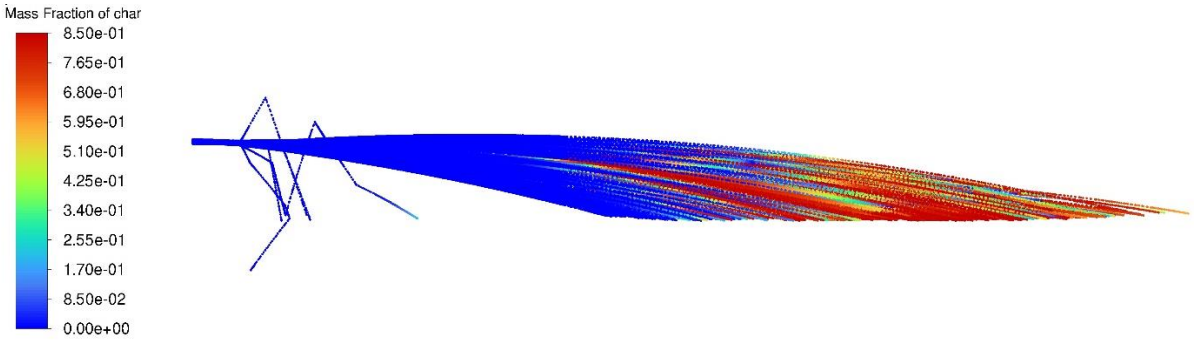


**Figure 13**: Char mass fraction distribution along particle trajectories, showing the gradual consumption of char through heterogeneous oxidation reactions until only inert ash remains.

## 4 CONCLUSIONS

A computational fluid dynamics (CFD) study was conducted to evaluate the feasibility of partially replacing natural gas with carbon-neutral biofuels in a rotary kiln. Biomass was modeled as multi-component particles undergoing drying, pyrolysis, and char oxidation, and their influence on the kiln's thermal environment was assessed. The comparison between the baseline case (natural gas only) and the co-firing case (10% biomass share) showed that the introduction of biomass led to a slight reduction in peak flame temperature, while the overall temperature distribution remained stable and sufficient to meet process requirements. Biomass particles followed the expected thermal conversion pathway of rapid heating, moisture release, pyrolysis, and progressive char oxidation, ultimately achieving complete burnout within the available residence time. The particle temperature increased consistently along its path, confirming effective coupling with the surrounding gas phase. Meanwhile, the solid bed temperature exhibited only minor differences between the two cases, with outlet values remaining within the desired operational range. Importantly, substituting 10% of the natural gas with biomass reduced fossil fuel consumption by the same fraction, thereby contributing to decarbonization objectives without compromising operational stability. Overall, the results confirm the technical feasibility of co-firing biomass at a 10% energy share in rotary kilns and highlight the value of CFD modeling as a predictive tool for advancing low-carbon industrial energy systems.

## 5 ACKNOWLEDGEMENTS

The authors gratefully acknowledge the financial support provided by K1-MET GmbH, the metallurgical competence center. This research was conducted within the framework of the K1-MET Competence Center, funded under the COMET – Competence Centers for Excellent Technologies – program by the Austrian Federal Ministry for Climate Action, Environment, Energy, Mobility, Innovation and Technology, and the Federal Ministry for Digital and Economic Affairs.

## REFERENCES

[1] I. Energy Agency, "Net Zero by 2050 - A Roadmap for the Global Energy Sector," 2021.
[2] Y. Zheng *et al.*, "Carbon Footprint Analysis for Biomass-Fueled Combined Heat and Power Station: A Case Study," *Agriculture (Switzerland)*, vol. 12, no. 8, Aug. 2022.
[3] R. Fernando, *Cofiring high ratios of biomass with coal*. 2012.
[4] S. Cant, "SB Pope, Turbulent Flows, Cambridge University Press, Cambridge, UK, 2000, 771 pp.," *Combust Flame*, vol. 125, no. 4, pp. 1361–1362, 2001.
[5] B. E. Launder and D. B. Spalding, "THE NUMERICAL COMPUTATION OF TURBULENT FLOWS," 1974.
[6] S. Chandrasekar, "Radiative Transfer Dover Publications," *New York*, 1960.
[7] B. F. Magnussen, "On the structure of turbulence and a generalized eddy dissipation concept for chemical reaction in turbulent flow," *American Institute of Aeronautics and Astronautics, Aerospace Sciences Meeting*, vol. 7, pp. 12–15, Jan. 1981.
[8] Kazakov A and Frenklach M, "DRM19," http://www.me.berkeley.edu/drm/.
[9] R. J. Kee, F. M. Rupley, and J. A. Miller, "Chemkin-II: A Fortran chemical kinetics package for the analysis of gas-phase chemical kinetics," Sandia National Lab.(SNL-CA), Livermore, CA (United States), 1989.
[10] S. Swaminathan, C. J. Spijker, and H. Raupenstrauch, "Numerical Modelling of An Industrial Rotary Kiln," 13th European Conference on Industrial Furnaces and Boilers, 2022.
[11] Y. Wang and C. M. Kinoshita, "KINETIC MODEL OF BIOMASS GASIFICATION," 1993.